Unconventional $T - H$ Phase Diagram in the Noncentrosymmetric Compound $Yb_2Fe_{12}P_7$

R. E. Baumbach,[1] J. J. Hamlin,[1] L. Shu,[1] D. A. Zocco,[1] J. R. O'Brien,[2] P.-C. Ho,[3] and M. B. Maple[1,*]

[1]*Department of Physics, University of California, San Diego, La Jolla, California 92093, USA*
[2]*Quantum Design, 6325 Lusk Boulevard, San Diego, California 92121, USA*
[3]*Department of Physics, California State University, Fresno, Fresno, California 93740, USA*

(Received 2 January 2010; published 1 September 2010; corrected 2 September 2010)

The temperature–(T-)magnetic-field (H) phase diagram for the noncentrosymmetric compound $Yb_2Fe_{12}P_7$, determined from electrical resistivity (ρ), specific heat (C), and magnetization (M) measurements on single crystal specimens, is reported. This system exhibits a crossover from a magnetically ordered non-Fermi-liquid (NFL) phase at low H to another NFL phase at higher H. The crossover occurs near the value of H where the magnetic ordering temperature (T_M) is no longer observable in $C(T, H)/T$ and $\rho(T, H)$, but not where T_M extrapolates smoothly to $T = 0$ K at a possible quantum critical point (QCP). This indicates the occurrence of a quantum phase transition between the two NFL phases. The lack of a clear relationship between the extrapolated QCP and NFL behavior suggests an unconventional route to the NFL ground states.

DOI: 10.1103/PhysRevLett.105.106403 PACS numbers: 71.27.+a, 05.30.Rt, 75.30.−m

The study of correlated electron physics has revealed deviations from Fermi liquid (FL) behavior in many d- and f-electron compounds based on elements with unstable valences [1,2]. For instance, non-Fermi-liquid (NFL) behavior is occasionally observed in the normal state properties of some materials, i.e., electrical resistivity $\rho(T) \sim T^n$ ($n < 2$), specific heat $C(T)/T \sim -\ln T$ or T^{-n} ($n < 1$), magnetic susceptibility $\chi(T) \sim -\ln T$ or T^{-n} ($n < 1$), and dynamical susceptibility $\chi''(T) = f(\omega/T)$ (where ω is the frequency) [3–7]. Several routes to NFL behavior have been proposed including Kondo disorder [8–10], Griffith's phase [11], quadrupolar Kondo [12], and quantum critical point (QCP) models [13–17].

The QCP model has been widely applied to situations where a second order phase transition, usually antiferromagnetic, is suppressed to $T = 0$ K by a control parameter (δ) such as chemical composition (x), pressure (P), or magnetic field (H), terminating in a QCP at $T = 0$ K. Order parameter fluctuations are manifested as NFL behavior at T's above the QCP, and a line emanating from the QCP delineates a gradual crossover from NFL to FL behavior at lower temperature and higher values of the control parameter. Extensive investigations of several prototypical systems (e.g., $CeCu_{6-x}Au_x$ [18] and $YbRh_2Si_2$ [19]) have been analyzed within the context of the QCP model and support the predicted "V-shaped" $T - \delta$ phase diagram.

We report measurements on single crystals of the ternary compound $Yb_2Fe_{12}P_7$, in which the Yb ions undergo magnetic ordering which is accompanied by an unconventional magnetic field tuned quantum ground state. This behavior is particularly interesting because it deviates strongly from the widely accepted QCP scenario described above, in that two NFL regions are observed, the first inside the magnetically ordered state and the second extending far beyond the extrapolated QCP as the tuning parameter H is increased. In particular, we find (1) a magnetically ordered ground state ($T_M \sim 0.9$ K) for which the signatures in electrical resistivity and specific heat measurements are suppressed to lower T with increasing H, (2) an NFL ground state for $T < T_M$ with a large $H = 0$ T electronic specific heat coefficient $\gamma(T) = C(T)/T$ that is suppressed with increasing H, and (3) a rapid crossover from the low H NFL state to another extended NFL region at the value of H where T_M can no longer be identified in the $C(H, T)$ and $\rho(H, T)$ data, which is stabilized for large values of H. These kinds of behavior suggest a quantum phase transition (QPT) between two phases that exhibit NFL behavior with different power law exponents of the electrical resistivity.

During our efforts to synthesize LnFePO and $LnFe_2P_2$ compounds, we found that $Ln_2Fe_{12}P_7$-type single crystals will often form in a Sn flux instead of the desired phase [20]. These compounds are members of a broad class of pnictogen-based systems with noncentrosymmetric structures and the chemical formula $Ln_{n(n-1)}T_{(n+1)(n+2)}M_{n(n+1)+1}$, where Ln is a lanthanide (or actinide), T is a transition metal, and M is a metalloid (phosphorus, arsenic) [21,22]. X-ray powder diffraction measurements reveal single phase samples with a hexagonal structure (space group $P\bar{6}$) and lattice parameters $a = 9.111$ Å and $c = 3.626$ Å, in agreement with earlier growth experiments where single crystals were synthesized in a Sn flux using only elemental starting materials [21]. In order to verify the stoichiometry, x-ray photoelectron spectroscopy measurements were performed, which revealed that Yb, Fe, and P are present in these crystals in a ratio consistent with the 2:12:7 formula.

The magnetic susceptibility $\chi(T) = M(T)/H$ [Fig. 1(a)] was measured for $T = 2$–300 K with $H = 0.1$ T applied both parallel and perpendicular to the c axis, using a Quantum Design (QD) Magnetic Properties Measurement

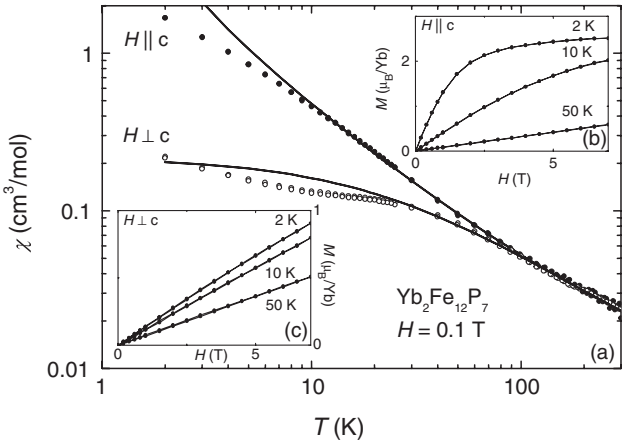

FIG. 1. (a) Magnetic susceptibility $\chi = M/H$ vs temperature T for magnetic field H applied perpendicular and parallel to the c axis. The solid lines are the CW fits to the data (see text). (b) M vs H for $H \parallel c$. (c) M vs H for $H \perp c$.

System. The $\chi(T)$ data reveal Curie-Weiss (CW) behavior where the effective magnetic moments ($\mu_{\text{eff}} = 4.1\mu_B$/Yb and $4.8\mu_B$/Yb for $H \parallel c$ and $H \perp c$, respectively) are close to the Yb^{3+} free ion value ($\mu_{\text{eff}} = 4.53\mu_B$/Yb) according to Hund's rules. The crystalline anisotropy is reflected in the CW temperatures (θ_{CW}) taken from fits to the data, for which $\theta_{\text{CW}} = 1$ K and -27 K for $H \parallel c$ and $H \perp c$, respectively. The $M(H)$ data [Figs. 1(b) and 1(c)] reveal that the c direction is the easy axis and the a or b directions are the hard axes. For $\chi_\perp(T)$, a CW law is observed down to $T \sim 30$ K, below which the data increase more weakly than expected from the high T CW behavior. The departure from CW behavior occurs near the onset of correlated electron phenomena inferred from the behavior of $C_p(T, H)$ and $\rho(T, H)$. A similar trend is observed for $\chi_\parallel(T)$ for $T < 10$ K.

The low T upturn in $\chi_\perp(T)$ below 10 K can be described by various functions, depending on whether the behavior is assumed to be extrinsic or intrinsic. In order to explore the first possibility, the data were fitted below 10 K with a modified Curie-Weiss law $\chi_\perp(T) = \chi_0 + C/(T - \theta)$, where χ_0 represents the contribution from nonmagnetic $Yb_2Fe_{12}P_7$ and the Curie-Weiss term is attributed to magnetic impurities. This fit yields the parameters $\chi_0 = 0.1$ cm^3/mol, $C = 0.3$ cm^3 K/mol, and $\theta = -0.6$ K. If the magnetic impurity is assumed to be Gd^{3+}, for which $\mu_{\text{eff}} = 7.94\mu_B B$, then this value for C would be equivalent to the occupation of 2% of the Yb sites by Gd^{3+}. However, this concentration is far too large for this to be a viable possibility. We also note that crystal misalignment with respect to H could be responsible for this behavior. On the other hand, assuming that the behavior is intrinsic and consistent with NFL behavior, we find that $\chi_\perp(T)$ can be described using either power law or logarithmic functions of the forms $\chi_\perp(T) = aT^{-n}$, where $a = 0.27$ cm^3 K^n/mol and $n = 0.32$, or $\chi_\perp(T) = b - c \ln T$, where $b = 0.25$ cm^3/mol and $c = 0.05$ cm^3/mol. From this analysis, we conclude this T dependence represents a departure from FL behavior.

The $H = 0$ T specific heat divided by temperature $C_p(T, H = 0)/T$ data, measured for $T = 50$ mK–300 K using a QD Physical Properties Measurement System (PPMS) and a QD ^{3}He-^{4}He dilution refrigerator (DR) [Fig. 2(d)], exhibit a broad peak near 120 K, which can be attributed to phonons. Below the peak, $C_p(T, H = 0)/T$ decreases down to $T \sim 10$ K, passes through a minimum, then increases rapidly, suggesting the formation of a strongly correlated electron ground state. A sharp peak is then observed [Fig. 2(b)], indicating that $Yb_2Fe_{12}P_7$ undergoes a phase transition near $T_M \sim 0.9$ K. With an applied magnetic field ($H \perp c$), this feature is completely suppressed by $H = 1$ T, although the large background upon which it is superimposed is barely affected. Since the phase transition is suppressed with H, we conclude that it likely includes an antiferromagnetic component. Below T_M, $C_p(T, H = 0)/T$ goes through a broad maximum where $C_{\text{max}}(T, H = 0)/T \sim 3.4$ J/mol Yb K^2 for $T \sim 0.27$ K, followed by a shallow minimum near 0.15 K, after which $C_p(T, H = 0)/T$ increases again for $T < 0.15$ K. For $H > 1$ T, $C_p(T, H)/T$ is suppressed and the location of the broad maximum shifts towards higher T. This behavior is consistent with an increase of the Zeeman energy with H and the recovery of a FL state.

We also note that the strong increase in $C_p(T)/T$ for $T < 10$ K could be due to a Schottky anomaly from

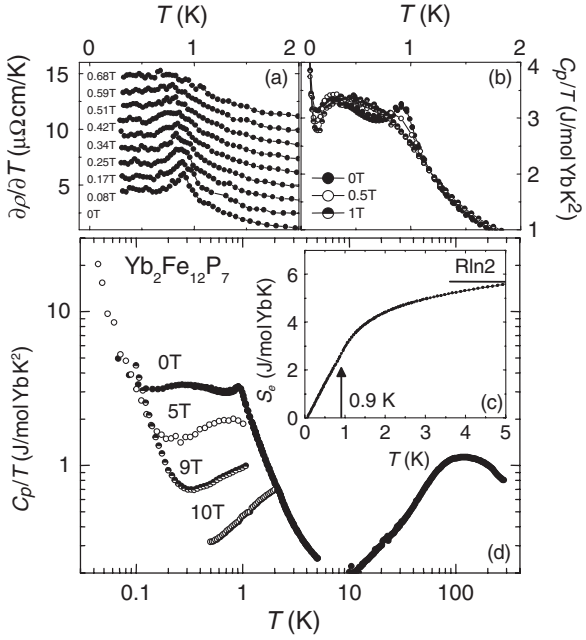

FIG. 2. (a) Derivative of the electrical resistivity with respect to temperature, $\partial\rho(T, H)/\partial T$. (b) Expanded view of specific heat divided by temperature $C_p(T, H)/T$ for $T < 2$ K and $H < 1$ T. (c) Electronic portion of the entropy $S_e(T, H = 0)$ for $T < 5$ K. (d) C_p/T vs T for several H.

crystalline electric field (CEF) splitting of the $J = 7/2$ Yb^{3+} multiplet. Assuming the ground and first excited states are doublets, the specific heat data should be described by the expression $C_p(T) = C_0 + C_{\rm Sch}(T)$, where $C_{\rm Sch}(T) = R(\Delta/T)^2 \exp\{(\Delta/T)/[1 + \exp(\Delta/T)]^2\}$, for which R is the ideal gas constant and Δ is the splitting between the doublets. If such a fit is performed for the $H = 1$ T data, we then find that $C_0 \approx 1345$ mJ/mol K and $\Delta \approx 2.2$ K. However, as shown in Fig. 2(c), the entropy $S(T, H = 0)$ only reaches a value of $R \ln 2$ near 5 K, which is too small to account for the entropy associated with both the magnetic ordering and the two level CEF energy scheme. Therefore, we exclude this scenario.

We last consider the low T upturn in C_p/T, which is consistent with a nuclear Schottky anomaly and can be described by the expression $C(T) = C_{\rm el} + C_2 T^{-2}$, where $C_{\rm el}$ and $C_2 T^{-2}$ are the electronic and nuclear contributions, respectively. If we plot $C(T)T^2$ vs T^3, it is possible to extract $C_2(H)$ from the $T = 0$ K intercepts. As expected for a nuclear Schottky anomaly, $C_2(H) = \alpha + \beta H^2$ ($\alpha \approx 1.14$ mJ K/mol and $\beta \approx 0.09$ mJ/mol K^2). In principle, Yb, Fe, or P nuclei could contribute to this term.

Shown in Fig. 3 are $\rho(T, H)$ data for $H \perp c$ which were measured in a four-wire configuration (for several samples) using a PPMS, an Oxford Kelvinox DR, and a QD DR for $T = 50$ mK–300 K. The $H = 0$ T electrical resistivity data decrease from room T, indicating metallic behavior down to $T \sim 50$ K. Below $T \sim 30$ K, $\rho(T, H = 0)$ evolves through a pronounced shoulder, which could be consistent

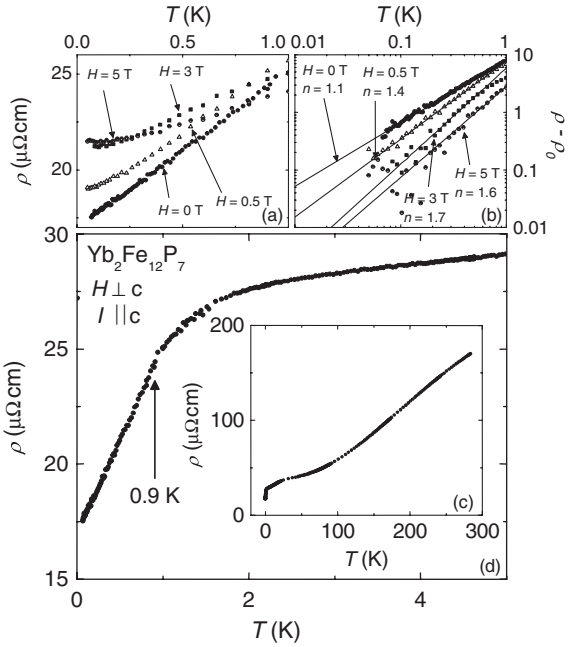

FIG. 3. (a) Electrical resistivity ρ vs temperature T for 0.05–1 K and magnetic fields $H \perp c$ axis. (b) $\rho - \rho_0$ vs T on a log-log plot. Fits are described in the text. (c) ρ vs T for $T =$ 0.05–290 K and $H = 0$ T. (d) ρ vs T for $T = 0.05$–5 K and $H = 0$ T.

with the two level Schottky anomaly scenario described above for $C_p(T)$, after which it decreases dramatically around $T_M \sim 0.9$ K. For $T < 2$ K, the $H = 0$ T measurements [Fig. 2(a)] reveal that $\partial\rho(T, H)/\partial T$ exhibits a maximum at $T_M \sim 0.9$ K. Most remarkably, $\rho(T, H = 0)$ is nearly linear for more than a decade in T below T_M [Fig. 3(a)]. By applying $H \perp c$, the maximum in $\partial\rho(T, H)/\partial T$ is suppressed and is no longer observable by $H \sim 0.7$ T. As expected for electron transport phenomena near a critical point where magnetic fluctuations are dominant, the shapes of $\partial\rho(T)/\partial T$ and $C_p(T)/T$ are similar and the resulting estimates for T_M from these two measurements are in good agreement [23]. To characterize $\rho(T, H)$ at low T, the data were fitted using the expression $\rho(T) = \rho_0 + AT^n$. The best fit was determined from a plot of $\ln(\rho - \rho_0)$ vs $\ln(T)$ in which the value of ρ_0 was selected to maximize the linear region of the fit extending from low T. Examples of these fits are shown in Fig. 3(b). The quantities ρ_0, A, and n are plotted in Figs. 4(a)–4(c), where ρ_0 increases and A decreases with increasing H. The behavior of n is discussed below.

Based on these measurements, it is possible to construct a $T - H$ phase diagram, as shown in Fig. 4(d). First, T_M decreases with H until it becomes impossible to track for $H > 0.7$ T. As a result, it is unclear whether there is a first order transition near 0.7 T or a second order transition in the vicinity of ~1.5 T, where we have extrapolated $T_M = 0$ K [dashed line in Fig. 4(d)]. The power law fits described above reveal that $n \sim 1.1$ for $H = 0$ T. As H is increased, n rapidly crosses over to a value ~1.5 near $H = 0.5$ T, close to the H where T_M is no longer observable. Starting near $H \sim 2.5$ T, the $n \sim 1.5$ dependence extends over an increasingly broad T region.

These results are striking, in light of the $C(T)/T$ data which are consistent with the recovery of a FL state with increasing H. In order to elucidate this point, we consider the Kadowaki-Woods ratio $R_{\rm KW} = A/\gamma^2$, which gives the relationship between the coefficient γ of the electronic specific heat and the coefficient A of the T^2 contribution to the electrical resistivity, assuming that the system exhibits heavy FL behavior; i.e., $C_p(T)/T \sim \gamma$ and $\rho(T) \sim T^2$ at low T. In the original treatment, $R_{\rm KW} \approx 10^{-5}$ $\mu\Omega$ cm(mol K^2/mJ)^2 [24]. More recently, it has been found that many (but not all) Yb based heavy fermion compounds follow the relationship $R_{\rm Yb} \approx 0.36 \times 10^{-6}$ $\mu\Omega$ cm(mol K^2/mJ)^2 [25]. From these quantities and the extrapolated $T = 0$ K values for γ (e.g., $\gamma \approx 2$ J/mol K^2 for $H = 5$ T), the coefficients $A_{\rm KW} \approx 40$ $\mu\Omega$ cm and $A_{\rm Yb} \approx 1.44$ $\mu\Omega$ cm (for $H = 5$ T) are found. For $A_{\rm KW}$, the expected FL contribution to $\rho(T)$ is much larger than the data. We thus rule out the possibility that $Yb_2Fe_{12}P_7$ is described by a simple heavy FL picture in the high H region. From $A_{\rm Yb}$, we find that the expected FL contribution to $\rho(T)$ is smaller than the data, suggesting that if this is the correct description, then it is necessary to

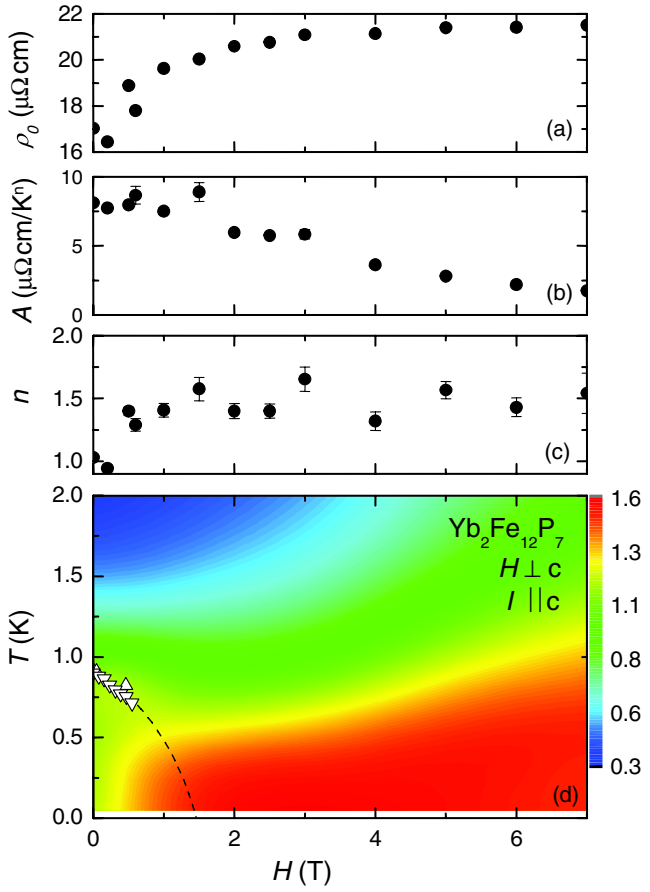

FIG. 4 (color online). (a)–(c) Magnetic field H dependence of the quantities ρ_0, A, and n from power law fits to the electrical resistivity data $\rho(T)$ (see text). (d) $T - H$ phase diagram for $Yb_2Fe_{12}P_7$. The values for T_M are taken from measurements of $C_p(T, H)$ (triangles) and $\rho(T, H)$ (upside-down triangles). The dashed line is an extrapolation of T_M to 0 K. The color gradient represents $\partial \ln(\rho - \rho_0)/\partial \ln T$, where ρ_0 maximizes the T range for the low T power law behavior for each $\rho(T, H)$. The values of $\partial \ln(\rho - \rho_0)/\partial \ln T$ above the low T fit range do not represent the local exponent n since they are based on ρ_0 values from the low T fits. Note that the low T power law fit range appears to be reduced from what would be inferred from Fig. 3(b). This is because the data are smoothed before taking $\partial \ln(\rho - \rho_0)/\partial \ln T$, resulting in a reduction of the apparent fit range because adjacent averaging samples the lower slope data above the upper T limit of the fit range.

invoke another hypothetical scattering process to account for the difference between the calculated and measured $\rho(T)$. Since T_M is suppressed near $H = 1$ T, there are no obvious candidates for the enhanced scattering. Therefore, we conclude that, although $C(T)/T$ suggests a return to FL behavior, $\rho(T)$ reveals persistent NFL behavior up to the highest H measured.

By comparison to classical QCP systems for which the NFL behavior is confined to a "V-shaped" region around the QCP, $Yb_2Fe_{12}P_7$ is anomalous. We emphasize that although there is a possible QCP, the ground state is disconnected from it and instead is more closely related to the H where T_M is no longer observable. This result suggests an unconventional ground state which includes a QPT between two phases that exhibit NFL behavior with different power law exponents of $\rho(T, H)$. Therefore, we conclude that $Yb_2Fe_{12}P_7$ belongs to a growing class of compounds in which the NFL behavior does not conform to the standard QCP scenario, strengthening the point of view that the interrelationship between NFL behavior and QCP or QPT phenomena is far from being understood. A particularly important question is whether the ubiquitous appearance of NFL behavior can be described universally or if it arises from a multitude of situations. This question applies to many correlated electron materials and its solution likely will be accompanied by a greater understanding of other related phenomena, such as high temperature and unconventional superconductivity.

Crystal growth and characterization were funded by the U.S. DOE under Grants No. DE FG02-04ER46105 and No. DE FG02-04ER46178. Low-temperature measurements were funded by the NSF under Grant No. 0802478.

*Corresponding author.
mbmaple@ucsd.edu

[1] M. B. Maple *et al.*, *Superconductivity: Conventional and Unconventional Superconductors* (Springer-Verlag, Berlin, 2008), Vol. 1, Chap. 13, pp. 639–744.
[2] M. B. Maple *et al.*, Physica (Amsterdam) **404B**, 2924 (2009).
[3] M. B. Maple *et al.*, J. Low Temp. Phys. **95**, 225 (1994).
[4] M. B. Maple *et al.*, J. Low Temp. Phys. **99**, 223 (1995).
[5] N. D. Mathur *et al.*, Nature (London) **394**, 39 (1998).
[6] G. R. Stewart, Rev. Mod. Phys. **73**, 797 (2001).
[7] G. R. Stewart, Rev. Mod. Phys. **78**, 743 (2006).
[8] O. O. Bernal *et al.*, Phys. Rev. Lett. **75**, 2023 (1995).
[9] E. Miranda *et al.*, J. Phys. Condens. Matter **8**, 9871 (1996).
[10] E. Miranda *et al.*, Phys. Rev. Lett. **78**, 290 (1997).
[11] A. H. Castro Neto, G. Castilla, and B. A. Jones, Phys. Rev. Lett. **81**, 3531 (1998).
[12] D. L. Cox, Phys. Rev. Lett. **59**, 1240 (1987).
[13] J. A. Hertz, Phys. Rev. B **14**, 1165 (1976).
[14] A. J. Millis, Phys. Rev. B **48**, 7183 (1993).
[15] T. Moriya *et al.*, J. Phys. Soc. Jpn. **64**, 960 (1995).
[16] Q. Si *et al.*, Nature (London) **413**, 804 (2001).
[17] P. Coleman *et al.*, J. Phys. Condens. Matter **13**, R723 (2001).
[18] H. v. Löhneysen *et al.*, Phys. Rev. Lett. **72**, 3262 (1994).
[19] O. Trovarelli *et al.*, Phys. Rev. Lett. **85**, 626 (2000).
[20] J. J. Hamlin *et al.*, J. Phys. Condens. Matter **20**, 365220 (2008).
[21] W. Jeitschko *et al.*, J. Solid State Chem. **25**, 309 (1978).
[22] Y. M. Prots *et al.*, Inorg. Chem. **37**, 5431 (1998).
[23] M. E. Fisher *et al.*, Phys. Rev. Lett. **20**, 665 (1968).
[24] K. Kadowaki *et al.*, Solid State Commun. **58**, 507 (1986).
[25] N. Tsujii, H. Kontani, and K. Yoshimura, Phys. Rev. Lett. **94**, 057201 (2005).